4

Diffusion Experiment in Lithium Ionic Conductors with the Radiotracer of [8]Li

Sun-Chan Jeong
Institute of Particle and Nuclear Studies (IPNS)
High Energy Accelerator Research Organization (KEK) 1-1 Oho
Japan

1. Introduction

Radioactive nuclides have been used in materials science for many decades. Besides their classical application as tracers for diffusion studies, nuclear techniques (i.e. Mössbauer Spectroscopy, Perturbed Angular Correlation, β-Nuclear Magnetic Resonance, Emission Channeling, etc.) are now being routinely used to gain microscopic information on the structural and dynamical properties of the bulk of materials via hyperfine interactions or emitted particles themselves (Wichert & Diecher, 2001). These nuclear techniques were primarily developed in nuclear physics for detecting particles or γ-radiations emitted during the decay of the radioactive nuclides. More recently these techniques have also been applied to study complex bio-molecules, surfaces, and interfaces (Prandolini, 2006). With the advent of most versatile 'radioactive isotope beam (RIB) factory' represented by the on-line isotope separator (ISOL)–based RIB facility (see Fig. 1), the possibilities for such investigations have been greatly expanded during the last decade (Cornell, 2003).

At the tandem accelerator facility of Japan Atomic Energy Agency (JAEA)-Tokai, a RIB facility, TRIAC (Watanabe et al., 2007)-Tokai Radioactive Ion Accelerator Complex- is operating since 2005. In the facility, short-lived radioactive nuclei produced by proton or heavy ion induced nuclear reactions can be accelerated up to the energy necessary for experiments. The energy is variable in the range from 0.1 to 1.1 MeV/nucleon, which is especially efficient for studies of the bulk of materials by using the RIBs as tracers. It allows us to implant (incorporate) the RIBs into specimens at a proper depth, avoiding the difficulties caused by the surface (e.g. diffusion barrier like oxide layers that often hampers the incorporation of those radioactive isotope probes into the materials of interest). In the facility, the separation and the implantation of radioactive probes are integrated into one device, as shown in Fig.1. Although the main concerns of the facility are nuclear physics experiments, as an effort to effectively use the available radioactive isotope beams at the TRIAC for materials studies, we have developed a diffusion tracing method by using the short-lived radioactive nuclei of [8]Li as diffusion tracers. The method has been successfully applied to measure diffusion coefficients in a typical defect-mediated lithium ionic conductor (refer to Chandra, 1981 for ionic conductors). We found that the present method is very efficient for the micro-diffusion, where the diffusion length is about 1μm per second.

In the following, the experimental method using ^{8}Li as a diffusion tracer and its application for measuring diffusion coefficients in inter-metallic lithium compounds will be reviewed, and then we will discuss possible extensions of the present method to study lithium diffusion with higher sensitivity such as the diffusion across interface in micrometer scale and the diffusion in nano-scale.
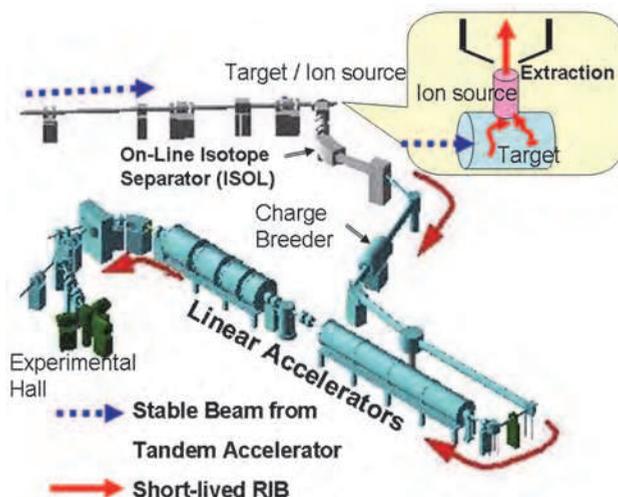

Fig. 1. Layout for ISOL-based RIB production at the TRIAC: Radioactive nuclei (e.g. uranium fission fragments) are produced by nuclear reactions induced in a thick target by a stable beam (e.g. UC$_2$ target by the irradiation of 30-MeV proton from the JAEA tandem accelerator which is not shown here). The target kept at a high temperature (~2000K) permits the fast diffusion of the reaction products into the ion source where they are ionized by plasma impact or surface ionization, as schematically shown in the inset. The singly charged ions (usually positively charged, 1+) are then extracted, mass-separated in a magnetic dipole field of the ISOL, and further, after being boosted to higher charge states by a charge breeder, accelerated to the energies necessary for experiments. For producing the radiotracer of ^{8}Li, the heavy ion beam of ^{7}Li on a ^{13}C-enriched graphite target was used (see the subsection 2-2).

2. Non-destructive on-line diffusion experiment

Over more than half a century, diffusion studies in solids using radioactive tracers (Tujin, 1997) have played an important role in understanding the underlying mechanism of atomic transport in solids, which is of great importance in a number of branches of materials science and engineering. Conventional diffusion studies by means of the radiotracer method in conjunction with a serial sectioning technique have been performed as follows (Wenwer at al., 1996): A small amount of a suitable radioactive isotope of the diffusing element is deposited onto the sample surface of interest. After a diffusion annealing at a temperature of T for a time of t, the sample is sectioned in parallel to the initial surface. An appropriate counting device measures the specific tracer activity in each section, which is proportional to the concentration of the diffusing species. The concentration-depth profile of the tracer is

then compared with the solution of Fick's second law under the experimental boundary conditions, yielding the tracer diffusion coefficient at the temperature T in the sample. The choice of an appropriate serial sectioning technique depends on the average diffusion length related to the annealing time and temperature, often by $2(Dt)^{1/2}$, where D is the tracer diffusion coefficient in the sample. The method is consequently destructive.

Although the conventional radiotracer method for diffusion studies has yielded the most accurate diffusion coefficients, the method has not yet been applied for some elements because of no-availability of radiotracers with adequate lifetimes (a rather long lifer time is needed for the process of annealing and sectioning). Among them, [8]Li, the radioactive isotope of Li with a half-life of 0.84 s is of special interest for practical issues; how well Li ions move in the secondary Li ion batteries. Fast Li diffusion is desirable in battery materials, i.e., Li ionic conductors for materials of electrodes and solid electrolyte. For studies on the macroscopic diffusivity of Li in Li ionic conductors, various electro-chemical methods (Sato et al., 1997) have been usually adopted up to now. However, the diffusion coefficients are scattered over several orders of magnitude, strongly depending on the method used for the measurement. Therefore, the diffusion coefficients measured in different ways, e.g., by using the radiotracer of Li, are highly required to settle down such disagreements. Such an experimental knowledge on the Li diffusion in as-developed materials for the battery is also of importance in the recent general efforts to design the battery by simulations based on the first principle.

2.1 Principle of the measurement of Li diffusion coefficients with the radiotracer of [8]Li

The radiotracer [8]Li decays through β-emission to [8]Be with a half lifetime of 0.84 s, which immediately breaks up into two α-particles with energies continuously distributed around 1.6 MeV with a full width at half maximum (FWHM) of 0.6 MeV (Bonner et al., 1948).

As for a diffusion tracer, special attention has been paid on the energy loss of the α-particles in the sample of interest, which is sensitive to the diffusion length of about 1 μm. In an ideal case when the radiotracer emits monochromatic α-particles, the amount of incidental energy loss of the α-particles on their passage to the surface of the solid of interest depends on the position of the decaying emitter; the measured energies of the α-particles passed through the solid are closely related to the decaying positions of the tracer. The time evolution of the energy spectra is therefore supposed to be a measure of the diffusivity of the tracer in the solid. The energy spectra are broadening with increasing diffusion time; the tracer diffusion coefficients could be simply obtained by the time-dependent widths of the measured energy spectra if the inherent energy of the emitted charged particles is well defined. In the present case, however, the inherent energy distribution of the α-particles is continuous and broad (Bonner et al., 1948). Although the correspondence between the emitted position and measured energy of the charged particles is not as simple as above, it was shown in the simulation that the tracer diffusion coefficient could be obtained from the time-dependent yields of α-particles emitted by diffusing [8]Li with the help of the simulation (Jeong et al., 2003).

Figure 2 shows schematically the principle of the measurement: Implanting the beam of [8]Li with a properly adjusted energy into a depth, which is deeper than the average range of α-particles, we can make a situation where most α-particles stop in the sample. After implantation, since the primary implantation profile is broadening by diffusion, the α-particles emitted by [8]Li diffused toward the surface can survive and come out of sample

with measurable energies. Then a charged particle detector located close to the sample surface could selectively detect α-particles from ^{8}Li diffusing toward the sample surface, since the implantation-depth is deeper than the average range of α-particles in the present case. Therefore, the temporal evolution of α-particle yields that come out of the sample would be a measure of the diffusivity of Li.

It should be noted that the present diffusion time is different from that of the conventional radiotracer method for diffusion studies (Wenwer at al., 1996) because the tracer in the present method diffuses all the time of the measurement. This is the reason why we call the present method as a non-destructive on-line measurement of diffusion.
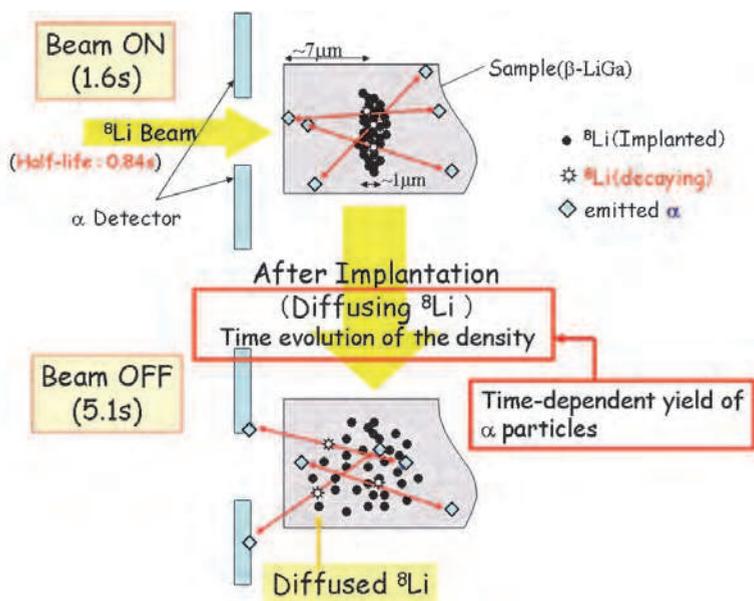

Fig. 2. Schematic view of the principle for measuring diffusion coefficients in β-LiGa (a typical sample of the inter-metallic Li compounds presently used) when the short-lived α-emitting ^{8}Li was used as the diffusion tracer. The yield of α particles measured at a time is a measure of the diffused distribution of ^{8}Li primarily implanted in the sample with a depth of about 7 μm.

2.2 Experimental set-up

Along the idea described in the previous subsection, we made an experimental set-up as shown in Fig. 3. All components were installed in a chamber evacuated to 1×10^{-4} Pa.

For producing ^{8}Li ($T_{1/2}$ = 838ms), we have used a neutron transfer reaction of ^{13}C (^{7}Li, ^{8}Li), using a sintered target of 99%-enriched ^{13}C. The 99%-enriched ^{13}C graphite disk (~10mm in diameter with a thickness less than 1mm) was mounted to the catcher position of the surface ionization type ion source with a beam window of 3-μm thick tungsten (Ichikawa et al., 2003). The target was bombarded with a 67-MeV ^{7}Li^{3+} beam with an intensity of about 100 pnA (particle nano-Ampere). The produced ^{8}Li was ionized, mass-separated as a radiotracer beam by the ISOL, and then injected to the post accelerators of the TRIAC, as shown in Fig.1.

Provide by the TRIAC, the radiotracer beam [8]Li of about 4 MeV with an intensity of about 10^4 particles/s was periodically implanted to a sample of β-LiGa with a following time sequence; 1.6 s for implantation (beam-on) and 5.1 s for subsequent diffusion (beam-off). With the incident energy, the [8]Li radiotracer can be implanted into the implantation-depth of about 7 μm from the front surface of the sample of β-LiGa. The α particles coming out of the sample were measured as a function of time by an annular solid-state detector (SSD) installed close to the front surface of the sample as shown in Fig. 3. The sequence was repeated to obtain good statistics, where the time-zero was always at the beginning of the implantation. Before starting the measurement, the sample was set at a temperature where the diffusion coefficient would to be measured.
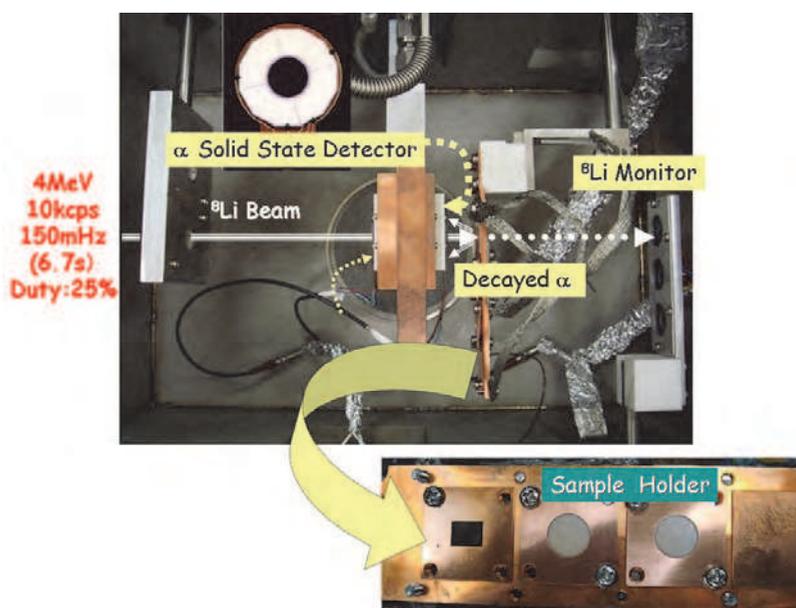

Fig. 3. Experimental set-up. The energetic and pulsed tracer beam of [8]Li provided by the TRIAC are implanted into the sample and the decayed α particles are measured as a function of time by the solid state detector located in front of the sample. The condition of the tracer beam is given, which includes energy, intensity, repetition frequency of the pulsed beam and its duty factor for the beam-on time.

2.3 Data analysis for diffusion coefficients

Using the experimental set-up in Fig. 3, a test experiment has been performed to measure the diffusion coefficients in the sample of LiAl compound (Jeong et al., 2005a, 2005b). Indeed, the diffusion coefficient of Li has been successfully obtained with an accuracy of better than 25% as a result of the comparison between the experimental and simulated time-dependent yields of α-particles. In the following, we present how diffusion coefficients are extracted in our present method, by applying to the measurement of the Li diffusion coefficients in LiGa, which is an inter-metallic Li compound and known as a good Li ionic conductor.

Figure 4 shows a normalized time spectrum of the yield of α-particles measured at room temperature for Li_xGa_{1-x}, x=0.54 in atomic ratio. The spectrum is presented by the ratios (i.e. time-dependent yields of α-particles divided by the α radioactivity of [8]Li at the time of interest). In this way was excluded the trivial time-dependency in the yield of α-particles just governed by the lifetime of [8]Li. The values of the ratios, therefore, should be constant over time if [8]Li does not diffuse at all. However, the experimental values as shown in Fig. 4 gradually increase with time and then fall off. Based on the relative time-dependency of α-particle yields (i.e. time dependent ratios), a diffusion coefficient was extracted by comparing with a Monte Carlo simulation where one-dimensional Fickian (Gaussian) diffusion was assumed. In Fig. 4 is also presented the time spectrum simulated with the diffusion coefficient best reproducing the experimental data as a result of comparisons to be described in the following.
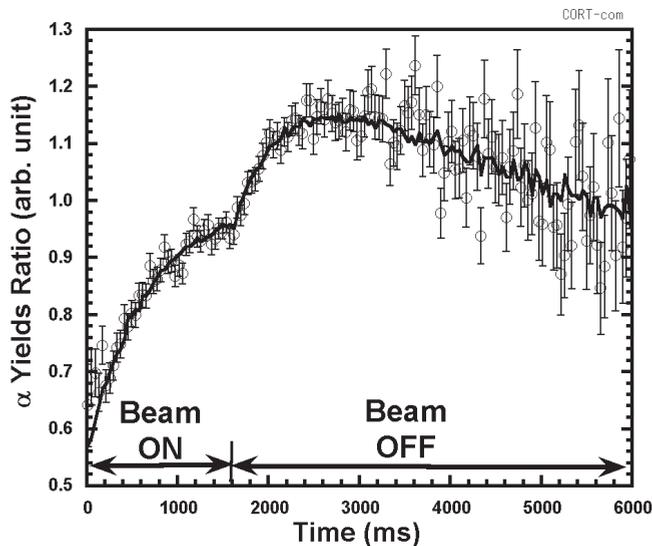

Fig. 4. Time spectrum of the α particle yields normalized by the α radioactivity of [8]Li implanted during the time of "Beam ON". The time spectrum, best simulated with the diffusion coefficient of $1.05 \times 10^{-7} cm^2/s$, is shown by solid line for comparison.

In the simulation, as described in detail in our previous publication (Jeong et al., 2003), we first defined the incident energy and energy spread of the [8]Li beam from the energy spectrum measured before implantation. Using the incident condition of the beam, we simulated the concentration-depth profile of [8]Li implanted in the sample and the time-evolution of the profile when a certain diffusion coefficient of Li in the sample was assumed. And then were simulated the energies of α-particles emitted from the time-dependent (diffusing) profiles of [8]Li, by taking into account the energy loss and straggling on their passage from the emitted position to the sample surface. Finally, integrated over the energies larger than 400 keV, the time-dependent α-particle yields associated with the diffusion coefficients assumed in the simulation were obtained and then compared with the experimental time spectrum, after being normalized in the same way as preformed for the

experimental data. It should be noted that the resultant is the macroscopic diffusion coefficients, since the simulation neglects the isotopic characters of diffusing elements. The parameters (mean and FWHM) describing the concentration-depth profile, and the energy loss and straggling of α-particles were estimated by using the SRIM-2003 code (Ziegler, 1985), which is widely used in this kind of application with high reliability.
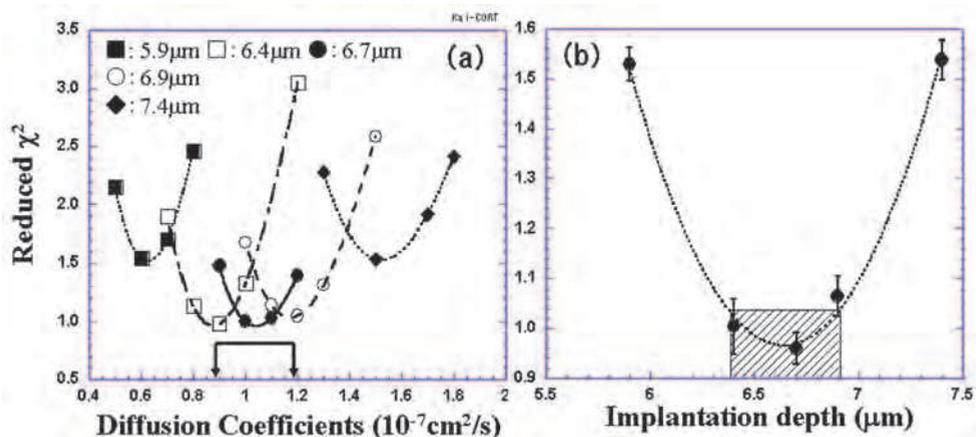

Fig. 5. (a) Reduced χ^2 values are compared for different implantation depths and correspondingly varied diffusion coefficients. Each of them was calculated with the spectrum simulated with a pair of implantation depth and diffusion coefficient. For each value of the implantation depth, the minimum value of the reduced χ^2 was extracted by a quadratic curve fitting as indicated by lines in (a), and then was plotted as a function of the corresponding depth in (b). By fitting the χ^2 values with a quadratic function of the depth [dotted line in (b)], the hatched region was estimated, especially as a constraint on the uncertain range of the implantation depth in the simulation. The allowed range of the depth was finally transformed into that of the diffusion coefficients [arrowed region in (a)], considering as a systematic error in the determination of the diffusion coefficient in the present case. (Fig. 2 from Jeong et al., 2008)

For comparison, we performed the χ^2 test, the likelihood test between the experimental and simulated time spectra. In the case of maximum likelihood, the reduced χ^2, the value of χ^2 simply divided by the number of data points in the present case, should be minimum and approximately close to 1. During the test of likelihood, two input parameters in the simulation were examined: diffusion coefficient and implantation depth. In the present simulation, the depth was explicitly considered as a variable input in order to take into account the roughness of the sample surface (less than 1μm) and range-uncertainty in the SRIM code. These two parameters were found to be most sensitive to the result of the simulation, i.e. the time-dependent structure of α-particle yields, but strongly inter-correlated in such a way that, e.g., simulations with somewhat higher (lower) diffusion coefficient and deeper (shallower) implantation could yield similar results as compared in Fig. 5(a). For different implantation depths, the χ^2 tests were explicitly performed with various diffusion coefficients. An example of the test is shown in Fig. 5(a), where the values of the reduced χ^2 were compared for different combinations of implantation depths and

diffusion coefficients assumed in the simulation. For a value of the implantation depth, a diffusion coefficient giving rise to maximum likelihood (minimum value of the χ^2) can be identified. The minimum values of the χ^2 and the corresponding implantation depths are further compared in Fig. 5(b). Then a pair of the implantation depth and the diffusion coefficient corresponding to the most minimum value of the reduced χ^2 in the comparison is finally obtained; the diffusion coefficient of $(1.05\pm0.15)\times10^{-7}$cm^2/s with the implantation depth of 6.64 (±0.25) μm in the present case. As indicated in Fig. 5 for the diffusion coefficients [arrowed in Fig. 5(a)] and implantation depth [hatched in Fig. 5(b)], the uncertainty in the determination of the coefficient comes mainly from the uncertain implantation depth. Here, we have considered the uncertain implantation depth as the main cause of systematic error inherent in the present method; otherwise the diffusion coefficient could be determined more accurately. It should be noted that the present results are not sensitive to the width of the primary concentration profiles of the tracer (Jeong et al., 2003).

As the reference spectrum for normalization, an experimental time spectrum of the α-radioactivity of ^{8}Li implanted in pure Cu was used. It allows us to avoid the systematic errors caused by the beam on/off operations, since no significant diffusion effects were observed in the case.

3. An application for measuring diffusion coefficients in Li ionic conductors

The β-phase of inter-metallic Li compounds, such as β-LiAl, LiGa and LiIn, has been considered as possible electrode materials in Li ionic batteries because of their high diffusion coefficients at room temperature for Li ions (Wen & Huggins, 1981). They are common in lattice structure; NaTl structure (Ehrenberg et al., 2002) composed of two interpenetrating sublattices, each forming a diamond lattice with a homogeneity range of around stoichiometric atomic ratio of Li (48~56 at. % Li for LiAl, 44~54% at. % Li for LiGa, 44~54 at. % Li for LiIn). In order to understand the motion of Li in the β phase as an ionic conductor, the defect structure in the Li compounds, closely related to the fast ionic motion, has been intensively studied via the measurement of electrical resistivity and density with help of the standard x-ray diffraction analysis (Sugai et al., 1995; Kuriyama et al., 1996). There exist three kinds of defects (see Fig. 6); vacancies on Li sites (V_{Li}), defects on anti-sites that replaced by Li (Li_A, A=Al, Ga, In) and complex defects (V_{Li} - Li_A). By forming the complex defects, the ionic motion of Li is suppressed or assisted depending on the kinds of anti-site atoms; Li diffusion rather slows down in β-LiAl while becomes rather faster in β-LiIn, although Li diffusivity almost linearly depends on the constitutional vacancy concentration on the Li sublattice (V_{Li}) (Tarczon et al., 1988). The high diffusion coefficient in the Li compounds is associated with the constitutional vacancy concentration on the Li sublattice, which is relatively large as compared to the usual metal alloy. The thermodynamic behavior of the Li vacancy has also been inferred from the anomalous electrical resistivity ("100K" anomaly) observed at around 95K near the critical composition corresponding to the Li-deficient region of β-LiAl (Kuriyama et al., 1980), which is considered as an order-disorder transition of vacancies on the Li sublattices (Brun et al., 1983).

The macroscopic ionic motion of Li has been so far inferred from the analysis of the electrical response to the applied voltage (electro-chemical method) (Sato et al., 1997). The values of diffusion coefficients, essentially obtained in such indirect ways, are often scattered over several orders of magnitude, strongly depending on the method of data analysis for finally extracting the diffusion coefficients.

Under such general situation, we have applied our method for measuring diffusion coefficients of Li, especially in β-LiGa where the diffusion coefficients has not been well measured although Li diffusion is known to be fastest among the Li inter-metallic compounds. The high diffusivity of Li in β-LiGa is associated with an especially large, constitutional vacancy concentration on the Li sublattice, almost three times lager than in β-LiAl. It would be also very interesting to observe, directly in terms of diffusion coefficient, the order-disordering transition of the vacancies on Li sites as well as the effect on the Li diffusion associated with the formation of the complex defects.
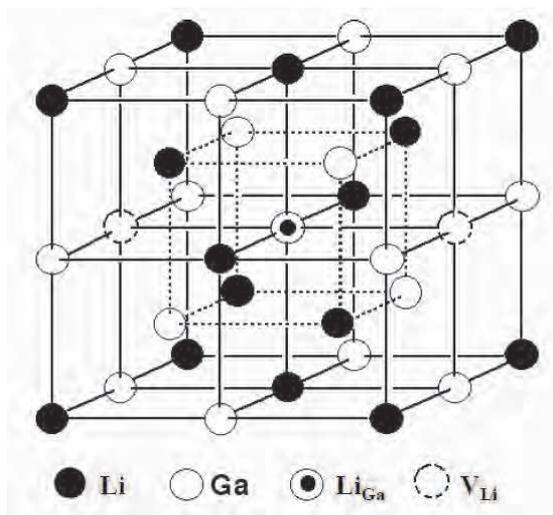
Fig. 6. Crystal structure of NaTl-type inter-metallic compound LiGa contained defects (Li: Li atoms at the Li-sites, Ga: Ga atoms at the Ga-sites, Li_{Ga}: Li atoms at the Ga-sites (i.e. anti-site defects, where Ga-sites are replaced by Li atoms), V_{Li}: vacancies at the Li-sites). The most Li-poor β-LiGa (44 at. % Li) can have two V_{Li} in unit cell, although the concentration of Li_{Ga} is close to zero (see Fig. 7).

3.1 Materials

The samples of β-LiGa with the Li composition of 43~54 at. % were prepared by direct reaction of desired amounts of lithium (99.9%) and gallium (99.999%) in a tantalum crucible. The crystallization was performed by the Tammam-stöber method as reported in Yahagi, 1980. And the crystal was found to be polycrystalline by X-ray diffraction analysis.

The composition of Li was determined by the electrical resistivity measurements, relying on the systematic correlation between them (Kuriyama et al., 1996) as shown in Fig. 7. The concentrations of the point defects, $[V_{Li}]$ and $[Li_{Ga}]$, strongly depends on Li compositions; with increasing Li composition from 43 to 54 at. %, $[V_{Li}]$ decreases from 11.4 to 2.8%, while $[Li_{Ga}]$ increases from 0 to 5.1%. V_{Li} is the dominant defect for Li-poor compositions, Li_{Ga} is the dominant defect for the Li-rich ones, and mixing of the two defects extends throughout the entire phase region. The coexistence of V_{Li} and Li_{Ga} is expected to form V_{Li}-Li_{Ga} complex defects (Kuriyama et al., 1996) as reported for the defect structure of β-LiAl (Sugai et al., 1995), which would play an important role in reducing the strain energy caused by the point

defects in the lattice matrix. Especially, almost the same amounts of V_{Li} and Li_{Ga} exist for the composition of about 51 at. % Li.
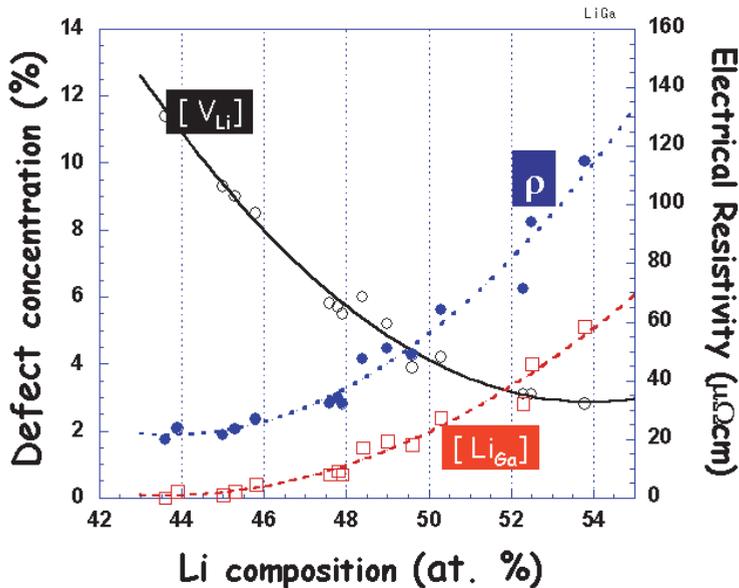

Fig. 7. Defect concentrations ($[V_{Li}]$, $[Li_{Ga}]$), electrical resistivity (ρ) vs. Li composition in atomic % for LiGa. The data points were taken from Kuriyama et al. 1996, and plotted for comparison.

The sample sliced in a form of disk with a diameter of 10mm and a thickness of 1mm was installed on the sample holder in the experimental chamber shown in Fig. 3. The surface of the sample was polished to the roughness less than 1 μm before set-up.

3.2 Li composition dependence of Li diffusion in Li inter-metallic compounds

Since the concentration of the defects is characterized by the Li composition under control in synthesis (Yahagi, 1980), as demonstrated in Fig. 7, the Li inter-metallic compounds have attracted much attention as a typical Li ionic conductor for investigating the high diffusivity of Li ions in a well-defined environment of defects. The detailed study on the diffusivity of Li in the Li inter-metallic compounds is further of interest, since the compounds have been considered as possible negative electrodes for Li ion secondary batteries more efficient than the commercially available (Wen & Huggins, 1981; Saint et al., 2005).

For β-LiAl and β-LiIn with the composition ranging between about 48 and 53 at. % Li, the diffusion coefficients of Li have been measured by a pulsed field gradient nuclear magnetic resonance (PFG-NMR) method in Tarczon et al., 1988, where was shown a strong correlation between the defect structure and the Li diffusion coefficient through their respective Li composition-dependency. The diffusion coefficient at room temperature was observed to become higher monotonously with decreasing Li composition - in other words, increasing concentration of V_{Li}. It was pointed out, furthermore, that the monotonous dependence of Li

diffusivity on the Li composition was found to be slightly modified, depending on the species of the anti-site atoms.

While the monotonous composition-dependence of Li diffusivity in both β-LiAl and β-LiIn strongly suggested that the Li atoms diffuse via a vacancy mechanism (i.e. by a vacancy-atom exchange process through nearest neighbored paths on the Li sublattice), the slight modification in the correlation was partly understood by the coexistence of two types of defects, namely vacancies in the Li sublattice and Li anti-site atoms in the aluminum or indium sublattice forming compound defects (V_{Li}-Li_{Al}, or V_{Li}-Li_{In}) (Kishio & Britain, 1979; Tarczon et al., 1988). Owing to the elastic relaxation of atoms against the strain induced in the vicinity of the point defects, the interaction between the two types of defects once forming a compound defect can be attractive or repulsive according to the relative size of the ions on the sublattice replaced by Li (atomic size effect). The Li anti-site atom Li_{Al} in β-LiAl produces compressional strain (expanded lattice), since the radius (0.68Å) for the Li ion in a closed shell configuration (Kittel, 2005) is larger than that (0.50 Å) for the aluminum ion, while the anti-site atom Li_{In} in β-LiIn induces dilatational strain (contracted lattice) because of ionic radius (0.8 Å) for indium larger than that of the substitutional Li ion. On the other hand, the vacancy V_{Li} always produces dilatational strain. Indeed, as supposed by the atomic size effect, the diffusion in β-LiIn was observed to be enhanced by the presence of the repulsive interaction between different types of defects, more than expected by the single vacancy diffusion mechanism (Tarczon et al., 1988).

Based on the atomic size effect, the interaction between V_{Li} and Li_{Ga} in β-LiGa is supposed to be attractive as in β-LiAl, because the radius (0.62 Å) of gallium ion is slightly smaller than that of Li ion. The strength of the interaction in β-LiGa is expected to be weaker than observed in β-LiAl and β-LiIn, since the radii of the constituent ions are quite close to each other. In addition to the specific interaction – attractive and weak, LiGa has stable β-phase over the Li composition range wider than investigated so far in β-LiAl and β-LiIn, consequently allowing us to address the Li diffusion in the concentration range of V_{Li} almost three times wider than before (Kuriyama et al., 1996).

The diffusion coefficients of Li in β-LiGa have not yet been measured in detail, but measured only by the electro-chemical method (Wen & Huggins, 1981), where the Li composition was not well defined. Using the on-line diffusion tracing method introduced in the previous section 2, we have measured the diffusion coefficients of Li in β-LiGa with the composition in the range of about 43 to 54 at. % Li. Of special interest is how the Li diffusion in β-LiGa depends on the Li composition, consequently the concentration of the V_{Li} defect.

3.2.1 Abnormal Li diffusion: Enhanced or suppressed by the formation of defect complex

In Fig. 8, the time-dependent normalized α-particle yields are compared for different Li compositions, i.e. 43.6, 50.0 and 53.2 at. % Li. Referring to the time dependence of the α-particle yields, the stoichiometric β-LiGa has the highest diffusivity of Li among three, most quickly rising and falling down. This observation is quite different from those observed for β-LiAl and β-LiIn (Tarczon et al., 1988) which are iso-structural with the β-LiGa.

The abnormal behavior of Li diffusivity in β-LiGa is well identified in Fig. 9, where the diffusion coefficients in β-LiGa at room temperature are presented as a function of Li composition together with the data for β-LiAl and β-LiIn reported in Tarczon et al., 1988. As shown in Fig. 9, the Li diffusion coefficients in β-LiAl and β-LiIn decrease monotonously

with increasing Li composition, but the correlation is changing due to the coexistence of vacant Li sites V_{Li} and anti-site Li atoms on the aluminum (or indium) sites Li_{Al} (or Li_{In}), as discussed earlier in terms of the size effect of constituent atoms. Assuming the single vacancy diffusion in LiGa, the diffusion coefficients are supposed to keep increasing in the Li-poor composition in similar ways as observed in both β-LiAl and β-LiIn. However, what observed in the present measurement goes the other way; the diffusion becomes faster around stoichiometric atomic ratio, i.e. showing a maximum around the Li composition of 48~50 at. %.
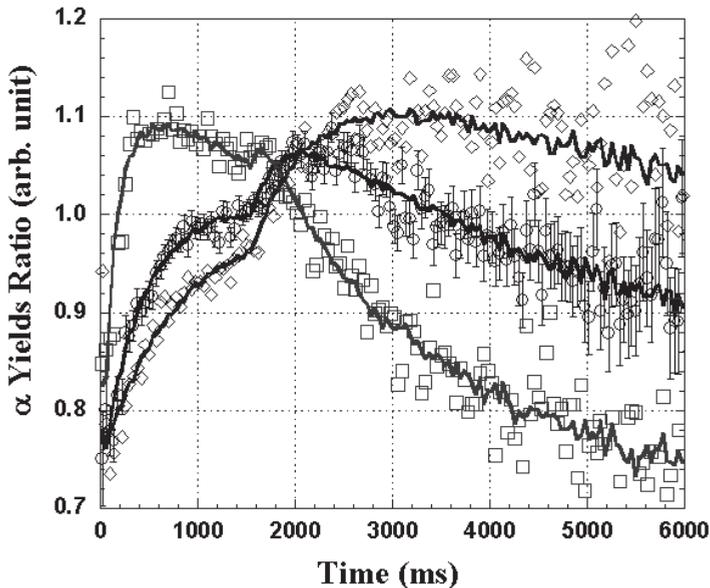
Fig. 8. Normalized time spectra of α yields obtained at room temperature for β-LiGa with Li atomic compositions of 43.6(○), 50.0(□) and 53.2(◇) at. %. The results from the simulation are also shown as solid lines. In the simulation, best reproducing the data as a result of χ^2 tests, the diffusion coefficients of $2.4 \times 10^{-7} cm^2/s$, $8.5 \times 10^{-7} cm^2/s$ and $1.2 \times 10^{-7} cm^2/s$ were assumed for 43.6, 50.0 and 53.2 at. % Li, respectively.

Although the data for β-LiAl and β-LiIn were available only in a limited range of Li composition from 48.3 to 53 at. % Li, it would be interesting to note that the diffusion coefficients in β-LiGa varied in a similar way (increase with decreasing Li content) between those values in β-LiAl and β-LiIn in the corresponding range of Li composition. This would be intuitively understandable, since the iso-structural β-LiGa with a comparable size of the constituent atoms should have an interaction between V_{Li} and Li_{Ga} with intermediate strength as compared to those discussed in the case of β-LiAl and β-LiIn. Therefore, the composition-dependence of Li diffusivity in β-LiAl and β-LiIn could be considered as the lower and upper limits of the Li diffusivity in β-LiGa over the Li composition range of interest, respectively; two complementary explanations might be possible by referring to the respective composition-dependency observed in β-LiAl and β-LiIn.

Referring to the tendency in β-LiIn, the diffusion of Li in very Li-poor β-LiGa seems to be suppressed. This could happen, for example, by assuming the formation of defect complex such as V_{Li}-V_{Li} and/or V_{Li}-Li_{Ga}-V_{Li}, since the concentration of V_{Li} become much (almost three times at maximum) larger (Kuriyama et al., 1996) in the more Li-poor composition than investigated in β-LiIn (Tarczon et al., 1988). It should be noted that the number of vacant Li sites in a unit cell volume (8 for Li and 8 for Ga) is about two for the most Li-poor β-LiGa (43.6 at. % Li), whereas there exist about one vacant Li site in every two-unit cells for the most Li-poor β-LiAl (48.3 at. % Li) and β-LiIn (48.4 at. % Li) (refer to Fig. 6). Here, we assumed the random distribution of the vacancies over the available sites.
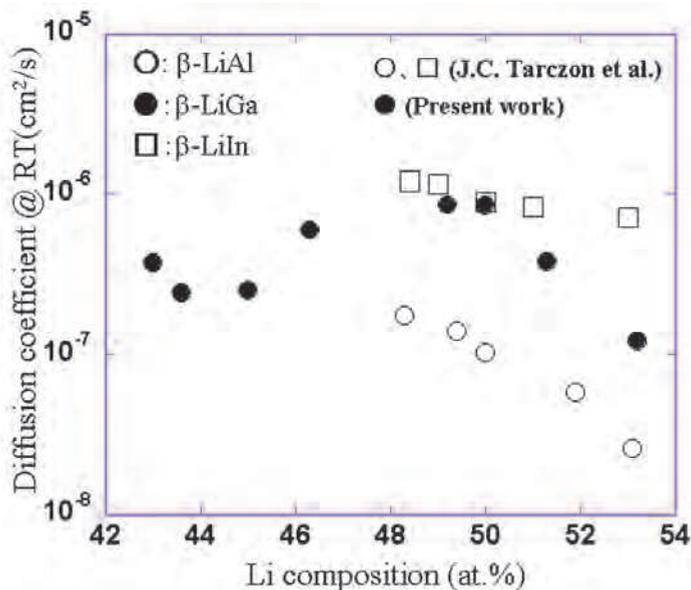
Fig. 9. Li composition-dependence of diffusion coefficients of Li at room temperature. The diffusion coefficients measured at room temperature are given as function of Li composition in atomic % for β-LiGa (present work), β-LiIn and β-LiAl (from Tarczon et al., 1988), respectively. The most Li-poor composition of LiGa shown in the figure is out of the β-phase (Fig.5 from Jeong at al., 2009).

Alternatively, assuming the diffusivity of Li in the most Li-poor β-LiGa as a good extension of the diffusivity of Li in the Li-poor β-LiAl (48.3 at. % Li) because of nearly zero concentrations of Li_{Al} and Li_{Ga} in the corresponding Li composition, the diffusivity of Li observed around the stoichiometric β-LiGa could be considered to be enhanced by the coexisting defects of V_{Li} and Li_{Ga}. Under the coexistence of V_{Li} and Li_{Ga}, the motion of the vacancies on the Li site, supposedly the carriers of Li atom, seems to be strongly promoted. This suggests that the interaction between V_{Li} and Li_{Ga} would be stronger and rather repulsive than expected by the atomic size effect, but not as strong as observed in β-LiIn. In addition, as a specific characteristic of the interaction in β-LiGa, we found strong composition-dependence of the interaction that appears to become stronger when a comparable amount of two types of point defects exists.

In the present measurement, although we found abnormal Li diffusion in very Li-poor composition of β-LiGa, the characteristic of the anomaly in diffusion, i.e. whether the diffusion is suppressed or enhanced, is not conclusive. A detailed theoretical consideration is highly required for quantitative discussion. From the experimental point of view, however, it would be interesting to extend the measurement to the more Li-poor composition of LiIn recently confirmed to have the β-phase in the same composition (Asano, 2000) as investigated for β-LiGa in the present work.

So far, we have compared our data for LiGa with those obtained by a pulsed field gradient nuclear magnetic resonance (PFG-NMR) method in Tarczon et al, 1988. The chemical diffusion coefficients of Li in LiGa obtained by an electrochemical method at 415°C were reported earlier (Wen & Huggins, 1981), where the self-diffusion coefficients of Li were also calculated by considering that the diffusivity of Ga was appreciably lower that that of Li. The self-diffusion coefficients at 415°C were found to be constant 1.1×10^{-6} and 5.0×10^{-7} cm^2/s on the Li poor and rich sides of LiGa, respectively, with a sudden change between 48 and 47.6 at. % Li. Those values were almost one order of magnitude smaller than those extrapolated to the temperature of 415°C from our present data. It should be noted that the similar amount of discrepancies in the values of diffusion coefficients were also found in the case of LiAl, by comparing the data obtained by PFG-NMR (Tarczon et al, 1988) and the electrochemical method (Wen et al, 1979).

3.3 Order-disordering of Li vacancies

Figure 10 shows time spectra of the yield of α-particles (represented by the ratios normalized to 1 at the end of beam-on) measured at different temperature for the stoichiometric LiIn. With decreasing temperature, the more α-particles are observed at later time, which means that the diffusion becomes slower at lower temperature. Interestingly, there observed a big change in the time structure of α-particle yields (normalized) at a certain temperature, where the temperature was varied by almost the same amount for the neighboring measurements compared in Fig. 10. Based on this relative time-dependency of α-particle yields (time dependent ratio) as demonstrated in Fig. 10, diffusion coefficients at various temperatures could be estimated by the way discussed previously.

In order to observe such a sudden change for β-LiGa, we have also performed a detailed measurement, where the temperature was varied by a fine step (about 5-degree difference in temperature between neighboring measurements), especially below room temperature.

The diffusion coefficients of Li in β-LiGa and β-LiIn with a near stoichiometeric composition of Li are displayed in Fig. 11 as a function of inverse temperature. For both samples, the diffusion coefficients suddenly change at a certain temperature, as observed time-dependent ratio spectra in Fig. 10, and follow Arrhenius behavior in the region of higher temperature. The sudden change in the value of the diffusion coefficient for β-LiGa of 44 at. % Li occurs at 234 (±2) K. The anomalous electrical resistivity (i.e. sudden change in the value of resistivity) is also observed at the same temperature, as shown in Fig. 11. The resistivity measurements were carried out using a van der Pauw method as used for β-LiAl (Sugai et al., 1995). This observation is closely related to the thermal properties of the structural defects, already observed as the anomalies in heat capacity (Hamanaka et al., 1998; Kuriyama et al., 1986) and nuclear-spin lattice relaxation (Nakamura et al., 2007) at 233 K near the critical composition of the Li-poor β-LiGa. It has been suggested that these phenomena are related to order-disorder transformation of the Li vacancies in the compounds. By the neutron

diffraction measurements for β-LiAl (Brun at al., 1983), a sudden change around 100K in the electrical resistance ("100K" anomaly as mentioned previously) has been understood by an ordering of the vacancies on the Li sublattice below the transition temperature; the structure below 100K is body centered tetragonal; the unit cell contains 10 Li and 20 Al positions, with the vacancies located at 2a positions.
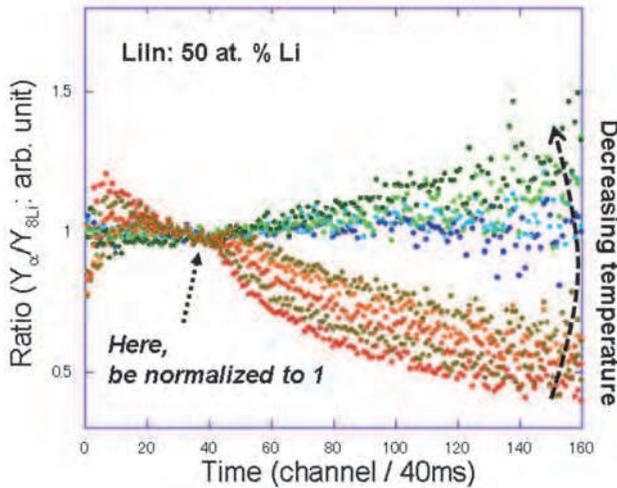

Fig. 10. Time spectra of α-particle yields measured at various temperatures for LiIn. The spectra were corrected for removing trivial time dependence and further normalized properly for easy comparison.
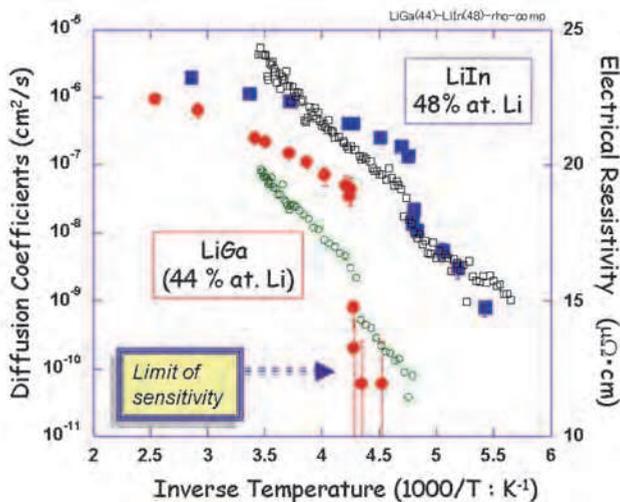
Fig. 11. Temperature-dependence of diffusion coefficients (closed symbols) and electrical resistivity (open symbols) for β-LiGa with 44 at. % Li, and β-LiIn with 48 % at. Li.

The ordering of the vacancies would produce a sharp drop in the Li diffusion coefficients at the ordering temperature, since the vacancies are supposed to be carriers of Li atom (i.e. ordered vacancies suppress the random exchange of Li atoms via vacancies). The observed amount of change, more than two orders of magnitude in the value of diffusion coefficients in the case of β-LiGa, is quite impressive as compared to those observed in the measurement of electrical resistivities where just a small change (at most 1/10) can be seen at the transformation temperature. The transition temperature is known to shift to lower temperature, and the change in the electrical resistivity becomes invisibly smaller with increasing Li composition, where a large fraction of the Li vacancies forms complex defects with anti-site Li atoms on Ga sublattices (Kuriyama et al, 1986). Therefore, with higher sensitivity, the present method could be applied for better investigating the characteristics of the transformation that are supposed to be correlated with the concentrations of structural defects (i.e. Li compositions).

Around the transition temperature, the time structure of the normalized α-particle yields could not be explained in terms of one component of diffusion, i.e. one diffusion coefficient, implying that the diffusion coefficients would not be singly determined in the transition region. The temperature window, in which the transition appears to occur, is about 10K.

At the lower temperature followed by a sudden change around 234 (±2) K for β-LiGa, the diffusion coefficients are observed as a constant, which is the lower limit of diffusion coefficients accessible by the present method; for diffusion coefficients less than about 10^{-10} cm^2/s, any significant effect in the yields of α-particles due to the diffusing ^{8}Li could not be observed because of the short life-time of the radiotracer.

4. Aiming at lithium micro- and nano- scope

As an extension of the present method, we consider the possibility to trace the Li macroscopic behavior across the interface in hetero-structural Li ionic conductors in micrometer scale, to be termed ^{8}Li microscope.

The time spectra shown in Fig. 10 represent dynamical movement of Li in the sample between as-implanted position and surface during a cycle for measurement. For a single layer (diffusion in homogeneous sample) as discussed in case of Fig.2, the present method can trace, most efficiently, the Li movement within one-dimensional distance of about 7μm for about 7s. For slow diffusion, Li is still moving toward the surface for the time of measurement, the α-particle yields are monotonically increasing with time. For moderate diffusivity, a maximum is observed when Li is reflected by the surface. After the maximum, the yield is simply decreasing with time since Li is diffusing into the bulk. For double layers (hetero-structural sample) whose interface exist in between, i.e. introducing an interface between the as-implanted position and the surface, we could observe time structure different from the case of single layer. In other words, we could observe how Li interacts with the interface, e.g. if Li is precipitated, perfect- or half-reflected on the interface. This idea could be applied to take a dynamical picture of Li in Li ion micro-batteries consisting of thin films of several μm in thickness. Therefore, the present method could be called ^{8}Li microscope by analogy with the neutron transmission image of Li in a secondary Li ion battery, where the picture of Li, actually ^{6}Li, in the battery was taken by the neutron radiography with a resolution of mm (Takai et al., 2005).
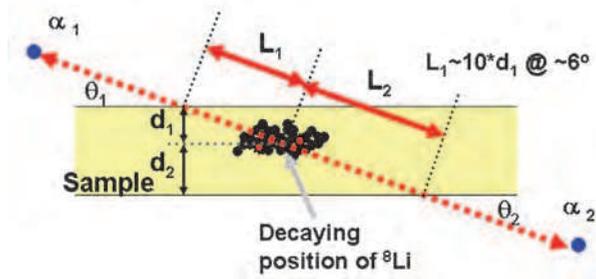
Fig. 12. Schematic layout for a coincident measurement of two α-particles emitted with angles of $\theta_1=\theta_2$ relative to the surface of sample. The actual path lengths (L_1 and L_2) in the sample are enhanced 10 times as compared to those considered in Fig. 2 when applying limitation to the emission angle of 6°.

For higher sensitivity, from micro-scale to nano-scale, we consider a coincident measurement of two α-particles emitted from position of β-decaying ^{8}Li. The micrometer sensitivity of the method discussed so far is partly coming from the broad energy distribution of α-particles on decaying. Therefore, the coincident measurement is supposed to dramatically improve the sensitivity since the coincident α-particles have the same energy at the decaying position. In diffusion tracing method by ^{8}Li, however, a special attention is paid on the energy loss of α-particles subjected to the actual path length in the sample of interest from the decaying to the detection positions. For diffusion in a nano-scale, the diffusion length is too short to give a significant change in the energy loss of α-particles. We further apply a limitation in emission (detection) angles to the coincident measurement as shown in Fig. 12. With small emission angles, the actual path length of α-particles in the sample of interest can be made significantly longer than implanted depth, giving rise to a considerable energy loss difference against a nano-scale diffusion length toward the surface.
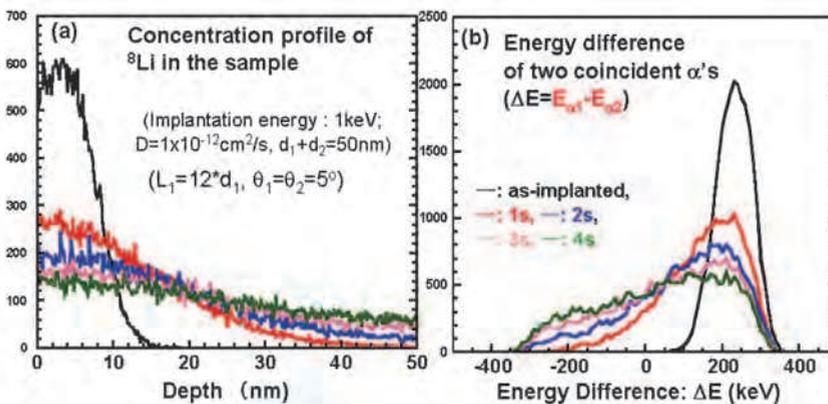

Fig. 13. (a) Simulated concentration profiles of ^{8}Li implanted into $LiCoO_2$ with a thickness of 50nm with an energy of 1keV and their evolution by diffusion simulated at 1, 2, 3 and 4 seconds after implantation with a diffusion coefficient of 10^{-12} cm^2/s. (b) Spectra of energy difference of α-particles coincidently emitted at angles of 5° relative to the surface of the sample. They are respectively simulated in the same time sequence as done in Fig.13 (a).

Along with the idea, we have performed a simulation to examine the feasibility and search for an observable most sensitive to diffusion profiles with a diffusion coefficient of 10^{-12} cm^2/s, a specific goal of present consideration. The simulation was performed in a similar way discussed in Jeong et al, 2003, by using the energy loss and straggling of α-particles provided by the SRIM-code. We assumed the diffusion coefficient as 10^{-12} cm^2/s, the sample thickness as 50nm, the emission angle as 5°, and the implantation energy as 1keV.

As a result of the simulation shown in Fig.13, we found that the energy difference between two coincidently measured α-particles could provide nano-scale sensitivity. The concentration profiles of ^8Li simulated sequentially with a condition given above are shown in Fig. 13 (a); the as-implanted profile is broadening with time by diffusion. Simulated in the same time sequence as done for profiles, the spectra of energy difference of two α-particles to be measured coincidently are compared in Fig. 13 (b). There is a good correspondence between the diffusion profiles and energy difference spectra, more specifically a clear one-to-one correspondence between decaying position of ^8Li and energy difference of two coincidently measured α-particles. For example, looking at the time evolution of the counts of coincident events with zero energy difference in the energy difference spectra should be a good measure of the time when ^8Li is across the middle of the sample, because the zero energy difference means that the path lengths experienced by two coincident α-particles are identical. We can conclude that the sensitivity against the diffusion of 10^{-12} cm^2/s could be easily achieved by the coincident measurement of two α-particles with the geometry assumed in the simulation.

5. Conclusions

A non-destructive and on-line radiotracer method for diffusion studies in lithium ionic conductors has been reviewed. As the tracer, the pulsed beam of the short-lived α-emitting radioisotope of ^8Li was implanted into a sample of interest. By analyzing the time-dependent yields of the α-particles from the diffusing ^8Li measured in coincident with the repetition cycle of the beam, the tracer diffusion coefficients were extracted with a good accuracy. The method has been successfully applied to measure the lithium diffusion coefficients in a typical defect-mediated lithium ionic conductor of LiGa, well demonstrating that the method is very efficient to measure the diffusion in the micro-meter regime per second. Anomalous composition-dependence of Li diffusion coefficients in β-LiGa was observed; the stoichiometric LiGa showed the highest diffusivity of Li. The anomaly was discussed qualitatively in terms of the formation of defect complex and the interaction between the constituent defects. The ordering of the Li vacancies in the Li-deficient LiGa was observed for the first time in terms of the Li diffusion by the present method, and its thermodynamic aspect was discussed. Further development, as an extension of the present method for higher sensitivity, was proposed to measure the diffusion on the nano-scale in lithium ionic conductors.

6. Acknowledgments

7. References

Bonner, P. W. et al. (1948). A study of breakup of ^{8}Li, *Physical Review*. Vol. 73, Issue 8, (April 1949), pp. 885-890, 0031-899X

Brun, T. O. et al. (1983). Ordering of Vacancies in LiAl, *Solid State Communications,* Vol. 45, Issue 8, (Feburary1983), pp. 721-724, 0038-1098

Chandra, S. (1981). *super-ionic solids: principle and applications*, North-Holland Publishing Company, ISBN 0-444-86039-8, New York

Cornell, J. (Ed.). (December 2003). Solid-Sate Physics at EURISOL, In: *The Physics Case for EURISOL*, GANIL, available from http://pro.ganil-spiral2.eu/eurisol/feasibility-study-reports/feasibility-study-appendix-a

Hamanaka, H. et al. (1998). Anomalous heat capacity and defect structure in β-LiGa, *Solid State Ionics*, Vol. 113-115, (December 1998), pp. 69-72, 0167-2738

Ichikawa, S. (2003). Ion source development for the JAERI on-line isotope separator, *Nuclear instruments & methods in physics research B*, Vol. 204, *(May 2003)*, pp. 372-376, 0168-583X

Ehrenberg, H. et al. (2002). Phase Transition from the Cubic Zintl Phase LiIn into a Tetragonal Structure at Low Temperature, *Journal of solid state chemistry*, Vol. 167, Issue 1, (August 2002), pp. 1-6, 0022-4596

Jeong, S. C. et al. (2003). Simulation Study on the Measurements of Diffusion Coefficients in Solid Materials by Short-lived Radiotracer Beams, *Japanese journal of applied physics*, Vol. 42, No. 7A, (July 2003), pp. 4576-4583, 0021-4922

Jeong, S. C. et al, (2005a). Measurement of diffusion coefficients in solids by the short-lived radioactive beam of ^{8}Li, *Nuclear Instruments and Methods in Physics Research B*, Vol. 230, Issues 1-4, (April 2005), pp. 596-600, 0168-583X

Jeong, S.C. et al. (2005b) Measurement of self-diffusion coefficients in Li ionic conductors by using the short-lived radiotracer of 8Li, *Journal of Phase Equilibria and Diffusion*, Vol. 26, No. 5, (September 2005), pp. 472-476, 1547-7037

Jeong, S.C. et al. (2008) On-Line Diffusion Tracing in Li Ionic Conductors by the Short-Lived radioactive Beams of 8Li, *Japanese journal of applied physics*, Vol. 47, No. 8, (July 2008), pp. 6413-6415, 0021-4922

Jeong, S.C. et al. (2009). Abnormal Li diffusion in b-LiGa by the formation of defect complex, *Solid State Ionics*, Vol. 180, Issues 6-8, (May 2009), pp. 626-630, 0167-2738

Kishio, K & Britain, J.O. (1979). Defect structure of β-LiAl, *Journal of Physics and Chemistry of Solids*, Vol. 40, Issue 12, (1979), pp. 933-940, 0022-3697

Kittel, C. (2005) *Introduction to Solid State Physics* (8-th ed.), Wiely, New York, p71

Kuriyama, K. et al. (1996). Defect Structure and Li-Vacancy Ordering in β-LiGa, *Physical review. B; Condensed matter and materials physics,* Vol. 54, Issue 9, (September 1996), pp. 6015-6018, 1098-0121

Kuriyama, K. et al. (1986). Electrical-transport properties in the semimetallic compound LiGa, *Physical review. B; Condensed matter and materials physics*, Vol. 33, Issue 10, (May 1986), pp. 7291-7293, 1098-0121

Kuriyama, K., Kamijoh, K & Nozaki, T. (1980). Anomalous Electrical Resistivity in LiAl Near Critical Composition, *Physical review. B; Condensed matter and materials physics*, Vol. 22, Issue 1, (July 1980), pp. 470-471, 1098-0121

Prandolini, M. J. (2006). Magnetic nanostructure: radioactive probes and recent developments, *Reports on Progress in Physics*, Vol.69, No. 5, (May 2006), pp. 1235-1324, 0034-4885

Nakamura K. et al. (2007). Li+ ionic diffusion and vacancy ordering in β-LiGa, *Faraday Discussions,* Vol. 134, (2007), pp. 343-352, DOI: 10.1039/B602445A

Saint, J. et al. (2005). Exploring the Li-Ga room temperature phase diagram and the electrochemical performance of the Li_xGa_y alloys vs. Li, *Solid State Ionics*, Vol. 176, issues 1-2, (January 2005), pp. 189-197, 0167-2738

Sato, H. et al, (1997). Electrochemical characterization of thin-film $LiCoO_2$ electrodes in propylene carbonate solutions, *Journal of Power Sources*, Vol. 68, Issue 2, (October 1997), pp. 540-544, 0378-7753

Sugai, H. et al. (1995) Defect Structure in Neutron-Irradiated b-6LiAl and b-7LiAl: Electrical Resistivity and Li Diffusion, *Physical review. B; Condensed matter and materials physics,* Vol. 52, Issue 6, (August 1995), pp. 4050-4059, 1098-0121

Takai S. et al. (2005). Diffusion coefficients measurements of La2/3-xLi3xTiO3 using neutron radiography, *Solid States Ionics*, Vol. 176, Issues 39-40, (September 2005), pp. 2227-2233, 0167-2738

Tarczon, J. C. et al. (1988).Vacancy-Antistructure Defect Interaction Diffusion in β-LiAl and β-LiIn, *Materials Science &. Engineering A,* Vol. 101, (May 1988), pp. 99-108, 0921-5093

Tuijn, C. (1997). On the history of Solid-state diffusion. *Defect and Diffusion Forum*, Vol. 141-142, (1997), pp. 1-48, 1662-9507

Yahagi, M. (1980). Single crystal growth of LiAl, *Journal of Crystal Growth*, Vol. 49, Issue 2, (June 1980), pp. 396-398, 0022-0248

Watanabe, Y. X. et al. (2007). Tokai Radioactive Ion Accelerator Complex (TRIAC), *European Physical Journal - Special Topics*, Vol. 150, No. 1, (March 2007), pp. 259-262, 1951-6355

Wen, C. J. & Huggins, R. A. (1981). Electrochemical Investigation of the Lithium-Gallium System, *Journal of The Electrochemical Society,* Vol. 128, issue 8, (August 1981), pp. 1636-1641, 0013-4651

Wen, C. J. et al. (1979). Thermodynamic and Mass Transport properties of "LiAl", *Journal of The Electrochemical Society,* Vol. 126, Issue 12, (December 1979), pp. 2258-2266, 0013-4651

Wenwer, F. et al. (1996). A universal ion-beam-sputtering device for diffusion studies, *Measurement science & technology*. Vol. 7, No. 4, (April 1996), pp. 632-640, 0957-0233

Wichert, T. & Deicher, M. (2001). Studies of semiconductors, *Nuclear Physics A,* Vol. 693, No. 3-4, (October 2001), pp.327-357, 0375-9474

Ziegler, J. F., Biersack, J. F. & Littmark, U. (1985). *The Stopping and Range of Ions in Solids* (2003 Version), Pergamon Press, New York, Chap. 8, available from http://www.srim.org/
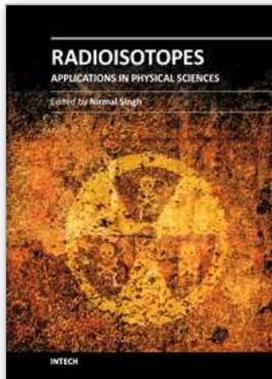
Radioisotopes - Applications in Physical Sciences

Edited by Prof. Nirmal Singh

ISBN 978-953-307-510-5

Hard cover, 496 pages

Publisher InTech

Published online 19, October, 2011

Published in print edition October, 2011

The book Radioisotopes - Applications in Physical Sciences is divided into three sections namely: Radioisotopes and Some Physical Aspects, Radioisotopes in Environment and Radioisotopes in Power System Space Applications. Section I contains nine chapters on radioisotopes and production and their various applications in some physical and chemical processes. In Section II, ten chapters on the applications of radioisotopes in environment have been added. The interesting articles related to soil, water, environmental dosimetry/tracer and composition analyzer etc. are worth reading. Section III has three chapters on the use of radioisotopes in power systems which generate electrical power by converting heat released from the nuclear decay of radioactive isotopes. The system has to be flown in space for space exploration and radioisotopes can be a good alternative for heat-to-electrical energy conversion. The reader will very much benefit from the chapters presented in this section.

INTECH
open science | open minds